

A hierarchical equations of motion (HEOM) analog for systems with delay: illustrated on inter-cavity photon propagation

Robert Fuchs¹ and Marten Richter^{1,*}

¹*Institut für Theoretische Physik, Nichtlineare Optik und Quantenelektronik, Technische Universität Berlin, Hardenbergstr. 36, EW 7-1, 10623 Berlin, Germany*

(Dated: January 9, 2023)

Over the last two decades, the hierarchical equations of motion (HEOM) of Tanimura and Kubo have become the equation of motion-based tool for numerically exact calculations of system-bath problems. The HEOM is today generalized to many cases of dissipation and transfer processes through an external bath. In spatially extended photonic systems, the propagation of photons through the bath leads to retardation/delays in the coupling of quantum emitters. Here, the idea behind the HEOM derivation is generalized to the case of photon retardation and applied to the simple example of two dielectric slabs. The derived equations provide a simple reliable framework for describing retardation and may provide an alternative to path integral treatments.

After the hierarchical equations of motion (HEOM) were initially invented by Tanimura and Kubo [1, 2] to solve numerically exactly the open quantum system problem with a Debye spectral density, the HEOM did not immediately take off, since the limited numeric capabilities did not allow for a versatile implementation at the time. However, the idea to use the time constant derivative of the Debye spectral density time correlation function stuck. Recently, various implementations [2–7] of HEOM followed after sufficient computing power became available. Soon after its invention, many generalizations using arbitrary spectral densities by decomposition into summed Debye form spectral densities were also developed. For most system-bath approaches it provides a well-established path to a numerically exact solution.

A different type of system-bath problem is the propagation of quantum states e.g. through a bath of photons or phonons [8–17]. A typical problem is describing quantum interconnects for quantum computing and cryptography applications. Recently, various applications of these systems with a delay caused by the propagation through the bath were investigated [8–17] including the development of different methods. However, the number of propagating photons is still limited, as it was for the open quantum systems approaches until HEOM implementations became widespread, along with other methods such as tensor networks [14, 15, 18–33]. In this paper, an analysis of the HEOM derivation in the context of delay is carried out and HEOM analog equations for systems with delay are derived. We demonstrate that the approach leads to a systematic set of equations ordered by the number of photons propagating through the bath. In the future, combinations with, e.g., tensor networks or automatic derivation may lead to an additional route to solve problems involving delays.

The paper starts with a derivation of the HEOM analog for open quantum systems with delay and illustrates its potential with a simple photon propagation example.

HEOM derivation: An HEOM analog with delay is

derived for an open quantum system with: $H = H_s + H_b + H_{sb}$. Here, H_s is the Hamiltonian of the system, which consists of quantum emitters in different spatially separated cavities. H_b is the bath Hamiltonian containing the propagating photon modes. Finally, H_{sb} is the system-bath coupling Hamiltonian. In open quantum systems, only the observables of the system are of interest, which can be calculated from the relevant density matrix $\rho_s(t) = \text{tr}_B(\rho(t))$. Its calculation is the main objective of HEOM, where we transfer the steps by Tanimura and Kubo [1] to systems with delay. We assume a factorized initial state $\rho(t_0) = \rho_s(t_0) \otimes \rho_B$, where ρ_B is a harmonic bath state. The system dynamics obey:

$$\begin{aligned} \rho_s(t) = & \text{tr}_B(T_{\leftarrow} U(t, t_0) \\ & \exp\left(-\frac{i}{\hbar} \int_{t_0}^t d\tau U(t_0, \tau) H_{sb,-}(\tau) U(\tau, t_0)\right) \\ & \rho_s(t_0) \otimes \rho_B), \end{aligned} \quad (1)$$

where $A_L \rho = A \rho$, $A_R \rho = \rho A$, and $A_- = A_L - A_R$ define the Liouville space operators acting on Liouville operator ρ for any Hilbert space operator A [34] and $U(t, t_0) = T_{\leftarrow} \exp\left(-\frac{i}{\hbar} \int_{t_0}^t d\tau (H_{s,-}(\tau) + H_{b,-}(\tau))\right)$ with time ordering operator T_{\leftarrow} . $H_{s,-}(\tau)$ may also contain Lindblad operators for describing external processes acting on the joint system-bath state. Following the HEOM derivation [1] and the path integral derivation from [17], we convert Eq. (1) to path integral form:

$$\begin{aligned} \rho_s(t) = & \text{tr}_B \left(\prod_{i=0}^M U_{i,i-1} \exp \left(\int_{t_0+\varepsilon(i-1)}^{t_0+\varepsilon i} d\tau U_{i-1}^\dagger(\tau) H_{sb,-}(\tau) U_{i-1}(\tau) \right) \right. \\ & \left. \rho_s(t_0) \otimes \rho_B \right) \end{aligned} \quad (2)$$

with $\varepsilon = (t - t_0)/M$ and $M \rightarrow \infty$ (in the following equations the limit is always assumed). Furthermore, $U_{i,j} = U(t_0 + \varepsilon i, t_0 + \varepsilon j)$ and $U_i(\tau) = U(\tau, t_0 + \varepsilon(i))$. For small ε , the approximation $U_{i,i-1} \exp \left(\int_{t_0+\varepsilon(i-1)}^{t_0+\varepsilon i} d\tau U_{i-1}^\dagger(\tau) H_{sb}(\tau) U_{i-1}(\tau) \right) \approx$

$U_{i,i-1} + \varepsilon \cdot U_{i,i-1/2} H_{sb}(t_0 + \varepsilon(i - 1/2)) U_{i-1/2,i-1} =: U_{i,i-1} + \varepsilon \cdot U_{sb}^{(1)}(i)$ holds, yielding:

$$\rho_s(t) = \text{tr}_B \left(T_{\leftarrow} \prod_{i=0}^M (U_{i,i-1} + \varepsilon \cdot U_{sb}^{(1)}(i)) \rho_s(t_0) \otimes \rho_B \right).$$

We assume linear system-bath coupling: $H_{sb} = \sum_{ij\mu} C_{ij\mu} A_{ij} B_\mu$ with system A_{ij} and linear bath operator B_μ . For a system A and bath B Liouville operator the relation $(AB)_- = A_+ B_- + A_- B_+$ holds, so $U_{sb}^{(1)}(i)$ can be written as a sum over products of the system and bath operators $U_{sb}^{(1)}(i) = \sum_l A_l^{(1)}(i) B_l^{(1)}(i)$, and we define $A_l^{(0)} = U_{i,i-1}^s \delta_{l,0}$ and $B_l^{(0)} = U_{i,i-1}^b \delta_{l,0}$ with the system and bath parts of $U_{i,i-1}$. With these relations, we write ρ_s in terms of a system part S and an influence functional (similar form as in [17]),

$$\rho_s(t) = \sum_{k_1 \dots k_M=0}^1 \sum_{l_1 \dots l_M} \left(\prod_{i=1}^M \varepsilon^{k_i} \right) S(k_1 l_1, \dots, k_M l_M) \times I(k_1 l_1, \dots, k_M l_M). \quad (3)$$

The system part is still an operator $S(k_1 l_1, \dots, k_M l_M) = T_{\leftarrow} \prod_{i=1}^M A_{l_i}^{(k_i)}(i) \rho_s(t_0)$, while the influence functional $I(k_1 l_1, \dots, k_M l_M) = \text{tr}_B(T_{\leftarrow} \prod_{i=1}^M B_{l_i}^{(k_i)}(i) \rho_B)$ is just a number. Since ρ_B is assumed to be a harmonic bath equilibrium state, Wick's theorem allows us to factorize the influence functional I into expectation values of two bath operators $B_l^{(1)}(\cdot)$. Furthermore, for small ε , the system propagator is roughly $U_{i,i-1}^s \approx Id_s - \frac{i}{\hbar} \varepsilon H_{s,-}(t_0 + \varepsilon(i - 1/2))$. Using the approximations of the time propagators

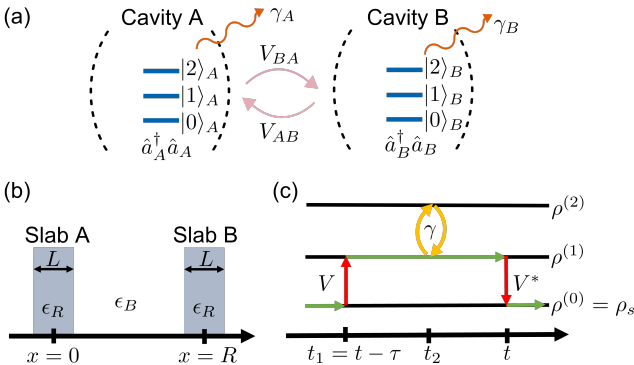


Figure 1. (a) Model of two open QNM cavities with dissipation rates γ_μ and effective inter-cavity coupling strength $V_{\mu\eta}$. (b) 1D model with two slabs of width $L = 21 \mu\text{m}$ with constant permittivity $\epsilon_R = \pi^2$ serving as QNM cavities, sitting against a background $\epsilon_B = 1$. (c) Scheme of the HEOM depicting a process including inter-cavity transfer and dissipation.

and using Wick's theorem we obtain,

$$\begin{aligned} \rho_s(t + \varepsilon) \approx & \rho_s(t) - \varepsilon \frac{i}{\hbar} H_{s,-}(t_0 + \varepsilon(M + 1/2)) \rho_s(t) \\ & + \sum_{l_{M+1}} T_{\leftarrow} \varepsilon A_{l_{M+1}}^{(1)} \sum_{k_1 \dots k_M} \sum_{l_1 \dots l_M} \left(\prod_{i=1}^M \varepsilon^{k_i} \right) A_{l_i}^{k_i}(i) \rho_s(t_0) \\ & \times \sum_{m=1}^M \text{tr}_B(B_{l_{M+1}}^{(1)}(M + 1) U_{M,m+1}^B B_{l_m}^{(1)}(m) \rho_B) \delta_{k_m,1} \\ & I(k_1 l_1, \dots, k_{m-1} l_{m-1}, 00, k_{m+1} l_{m+1}, \dots, k_M l_M), \end{aligned}$$

including only the terms at most linear in ε . Collecting the terms linear in ε yields the derivative of ρ_s [1]:

$$\begin{aligned} \partial_t \rho_s(t) = & -\frac{i}{\hbar} H_{s,-}(t) \rho_s(t) \quad (4) \\ & + \sum_{l\bar{l}} A_l^{(1)}(t) \int_{t_0}^t dt_1 \langle B_l^{(1)}(t) B_{\bar{l}}^{(1)}(t_1) \rangle_B \rho_{s\bar{l}}^{(1)}(t, t_1), \end{aligned}$$

where $\langle A \rangle_B = \text{tr}_B(A \rho_B)$ and the bath correlation function is in the interaction picture, and

$$\begin{aligned} \rho_{s\bar{l}}^{(1)}(t, \tilde{t}) = & \delta_{k_m,1} \delta_{l_m,1} \left\langle T_{\leftarrow} \prod_{i=1, i \neq m}^M B_{l_i}^{(k_i)}(i) \right\rangle_B \\ & \sum_{k_1 \dots k_M} \sum_{l_1 \dots l_M} T_{\leftarrow} A_l^{(1)}(m) \left(\prod_{i=1, i \neq m}^M \varepsilon^{k_i} A_{l_i}^{(k_i)}(i) \right) \rho_s(t_0), \end{aligned}$$

with $\tilde{t} = m\varepsilon + t_0$. Here, the derivation deviates from the original recipe of Kubo and Tanimura, since the assumption of a spectral density in Debye form (simple exponential $e^{-\gamma t}$ in time) is not compatible with systems including delay. Generalizations of HEOM usually rely on a decomposition of the spectral density into a sum of exponential functions to recover the Debye form. However, an expansion of the correlation function for the delay case using $e^{-\gamma|t-t_{\text{delay}}|}$ does not yield the advantages of Kubo's and Tanimura's approach, since the original relies on a time constant derivative of the Debye spectral density time correlation function. Instead, a delayed correlation of the above form introduces a sign change at $t = t_{\text{delay}}$, so that a dependence of $\rho^{(n)}$ on earlier integration times is unavoidable in the case with delay. Thus the integration over t_1 is not included in the definition of $\rho^{(1)}$ in contrast to the original HEOM [1]. Keeping the general form of the bath correlation function is more flexible than using a special form, which would simplify the equations of motion in the following. $\rho_{s\bar{l}}^{(1)}(\cdot, t_1)$ describes bath disturbances to the system density matrix, which are initially caused by an interaction with $A_{\bar{l}}^{(1)}$ at time t_1 (similar to the auxiliary dimensions in extended TCL [35]). Of course, the additional time argument prevents direct numerical implementations for increasing n . But specific bath correlation functions together with analytic calculation or tensor network methods [14, 15, 29–33, 36–40] will allow solutions nevertheless. Using the

same technique as for $\partial_t \rho_s(t)$ yields:

$$\begin{aligned} \partial_t \rho_{sl_1}^{(1)}(t, t_1) &= -\frac{i}{\hbar} H_{s,-}(t) \rho_{sl_1}^{(1)}(t, t_1) \\ &+ \sum_{l_2 \tilde{l}_2} A_{l_2}^{(1)}(t) \int_{t_0}^t dt_2 \langle B_{l_2}^{(1)}(t) B_{\tilde{l}_2}^{(1)}(t_2) \rangle_B \rho_{sl_1 \tilde{l}_2}^{(2)}(t, t_2, t_1) \\ &+ \delta(t - t_1) A_{l_1}^{(1)}(t_1) \rho_s(t_1 - 0^+). \end{aligned} \quad (5)$$

where we use the interaction picture for the bath correlation function. Instead of an initial condition $\rho_{sl_1}^{(1)}(t_1, t_1) = A_{l_1}(t_1) \rho_s(t_1 - 0^+)$, the δ term at the time of the initial condition is included. I.e., $\rho_{sl_1}^{(1)}(\cdot, t_1)$ is equal to zero (in the delta case) or not defined (in the initial condition case) before time t_1 . Note that t_1, t_2 of $\rho^{(2)}(t, t_2, t_1)$ are not time ordered since different delay/retardation times can occur in open quantum systems.

The form of $\rho^{(2)}$ points to a general definition of $\rho^{(n)}$ starting with $\rho^{(0)}(t) = \rho_s(t)$:

$$\begin{aligned} \rho_{sl_1 \dots \tilde{l}_n}^{(n)}(t, \tilde{t}_n, \dots, \tilde{t}_1) &= \\ &\sum_{k_1 \dots k_M} \sum_{l_1 \dots l_M} T_{\leftarrow} \left(\prod_{j=1}^n A_{\tilde{l}_j}^{(1)}(m_j) \delta_{\tilde{l}_j, l_{m_j}} \delta_{\tilde{k}_{m_j}, 1} \right) \\ &\left(\prod_{j=1, \wedge_{i=1}^n j \neq m_i}^M \varepsilon^{k_j} A_{l_j}^{(k_j)}(j) \right) \rho_s(t_0) \\ &\left\langle T_{\leftarrow} \prod_{j=1, \wedge_{i=1}^n j \neq m_i}^M B_{l_j}^{(k_j)}(j) \right\rangle_B, \end{aligned} \quad (6)$$

with $\tilde{t}_i = m_i \varepsilon + t_0$. Analogous to $\rho^{(1)}$, this yields:

$$\begin{aligned} \partial_t \rho_{sl_1 \dots l_n}^{(n)}(t, t_1, \dots, t_n) &= -\frac{i}{\hbar} H_{s,-}(t) \rho_{sl_1 \dots l_n}^{(n)}(t, t_1, \dots, t_n) \\ &+ \sum_{l_{n+1} \tilde{l}_{n+1}} A_{l_{n+1}}^{(1)}(t) \int_{t_0}^t dt_{n+1} \langle B_{l_{n+1}}^{(1)}(t) B_{\tilde{l}_{n+1}}^{(1)}(t_{n+1}) \rangle_B \\ &\rho_{sl_1 \dots l_n \tilde{l}_{n+1}}^{(n+1)}(t, t_1, \dots, t_{n+1}) \\ &+ \sum_{p=1}^n \delta(t - t_p) A_{l_p}^{(1)}(t_p) \\ &\times \rho_{sl_1 \dots l_{p-1} l_{p+1} \dots l_n}^{(n-1)}(t_p - 0^+, t_1, \dots, t_{p-1}, t_{p+1}, \dots, t_{n+1}). \end{aligned} \quad (7)$$

The last term is again a replacement to an initial condition: $\rho_{sl_1 \dots l_n}^{(n)}(t_p, t_1, \dots, t_n) = A_{l_p}(t_p) \rho_{sl_1 \dots l_{p-1} l_{p+1} l_n}^{(n-1)}(t_p - 0^+, t_1, \dots, t_{p-1}, t_{p+1}, \dots, t_n)$ with $t_p = \max_i(t_i)$, and it is clear that $\rho_{sl_1 \dots l_n}^{(n)}(t, t_1, \dots, t_n) = 0$ for $t < t_p$. So for the last term only p with the largest time t_p contributes. Furthermore $\rho_s^{(n)}$ is invariant under permutations of t_1, \dots, t_n including their corresponding l_1, \dots, l_n .

The physics behind Eq. (7) is very accessible: n corresponds to the maximum number of photons traveling in the bath at a given time t , so an exact truncation of

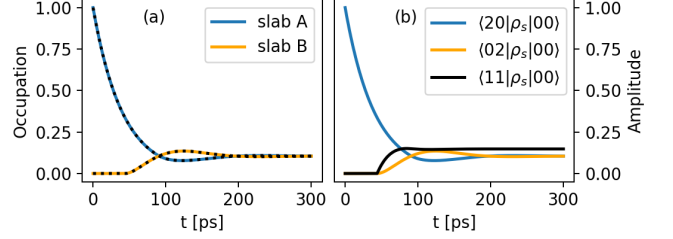


Figure 2. (a) Single-photon occupations of the two 1D dielectric slabs from Fig. 1. The dotted lines show the full reference wave function solution. (b) Absolute values of the two-photon coherences. For both cases, the QNM frequencies of the slabs are identical $\tilde{\omega}_1 = (0.06 - 0.0124i)$ eV, with coupling strength $V_{BA} = V_{AB} = 0.0062$ eV.

the equations based on the traveling photons is possible. Note, the photons on the left and right side states of the density matrix count accumulating, so a transfer of a single photon density requires two traveling photons (left and right side of density matrix), as opposed to one traveling photon for a single photon coherence. For other open quantum system equations of motion techniques such as Nakajima-Zwanzig [41] or time convolution less (TCL) equations [41], the generators \mathcal{K} in the equations of motion contain the system-bath coupling in any order. A calculation of higher-order contributions from \mathcal{K} is generally cumbersome involving higher products of system-bath correlation functions as well as a truncation at a given photon number. For the HEOM analog, only one system-bath correlation function appears in the second term of Eq. (7) cleanly separating on photon number. The first term of Eq. (7) describes the system dynamics. The second term represents the absorption of a bath photon, which entered the bath at time t_{n+1} . The last term describes photon emission into the bath.

Two photon propagation: As a benchmark for the new approach, we consider two spatially separated quasinormal mode (QNM) cavities, coupled to a common photonic bath (Fig. 1(a)). The QNMs \tilde{f}_μ are an open system analog to normal modes, which solve the Helmholtz equation under an outgoing radiation condition [42–48]. QNMs have complex eigenfrequencies $\tilde{\omega}_\mu = \omega_\mu - i\gamma_\mu$ with photon decay rate $\gamma_\mu > 0$. Here, two dielectric slabs serve as QNM cavities as in Fig. 1(b). We assume an effective 1D problem with homogenous continuation in the y, z direction. The model allows the analytical calculation of the modes (assuming a constant real permittivity ϵ_R) and coupling elements (cf. [49]). We include only the lowest energy QNM, assuming that all other modes are off-resonance. Since the slabs are identical, both have the same frequency $\tilde{\omega}_A = \tilde{\omega}_B = \tilde{\omega}_1$. However, we keep the indices for generality. The slabs are separated by the distance R , which is large enough for a separate quantization of the modes without inter-cavity coupling.

As a first step, we consider a population with initially

one excitation (one photon on each side of the density matrix) in slab A and a vacuum bath. Therefore, the hierarchy truncates at $n = 2$, i.e. $\rho^{(n)} = 0, n > 2$, and:

$$\begin{aligned} \rho_{s,l_1,l_2}^{(2)}(t, t_1, t_2) = & \\ & \Theta(t_1 - t_2) U^s(t, t_1) A_{l_1}^{(1)}(t_1) \rho_{s,l_2}^{(1)}(t_1 - 0^+, t_2) \\ & + \Theta(t_2 - t_1) U^s(t, t_2) A_{l_2}^{(1)}(t_2) \rho_{s,l_1}^{(1)}(t_2 - 0^+, t_1), \quad (8) \end{aligned}$$

using the initial conditions for $\rho^{(2)}$. *The truncation is exact* since the maximal number of propagating photons at any time is set by the initial conditions.

Inserting Eq. (8) into Eq. (5), we obtain:

$$\begin{aligned} \partial_t \rho_{sl_1}^{(1)}(t, t_1) = & -\frac{i}{\hbar} H_{s,-}(t) \rho_{sl_1}^{(1)}(t, t_1) \\ & + \sum_{l_2 \tilde{l}_2} A_{\tilde{l}_2}^{(1)}(t) \int_{t_0}^{t_1} dt_2 \langle B_{\tilde{l}_2}^{(1)}(t) B_{l_2}^{(1)}(t_2) \rangle_B \\ & \times U^s(t, t_1) A_{l_1}^{(1)}(t_1) \rho_{sl_2}^{(1)}(t_1 - 0^+, t_2) \\ & + \sum_{l_2 \tilde{l}_2} A_{\tilde{l}_2}^{(1)}(t) \int_{t_1}^t dt_2 \langle B_{\tilde{l}_2}^{(1)}(t) B_{l_2}^{(1)}(t_2) \rangle_B \\ & \times U^s(t, t_2) A_{l_2}^{(1)}(t_2) \rho_{sl_1}^{(1)}(t_2 - 0^+, t_1) \\ & + \delta(t - t_1) A_{l_1}^{(1)}(t_1) \rho_s(t_1 - 0^+). \quad (9) \end{aligned}$$

Eqs. (9) and (4) form a closed set of equations of motion for the system density matrix that are exactly solvable (cf. [49]) for at most two traveling photons. Fig. 1(c) illustrates connections between the equations with one photon traveling from time $t_1 = t - \tau$ until t through the bath, requiring the calculation of $\rho^{(1)}$. Intermittently a second photon is emitted into the bath at t_2 .

The dynamics of a specific system are determined by the system-bath correlation function $\text{tr}_B(B_{\tilde{l}_2}^{(1)}(t) B_{l_2}^{(1)}(t_1) \rho_B)$, which describes the emission of a photon into the bath at time t_1 and reabsorption at time t . The correlation function results from the system-bath coupling and reads (cf. [49]):

$$\begin{aligned} C_{\mu\eta}(t - t') \approx & 2V_{\mu\eta}\hbar^2 (\Theta(t - t')\delta(t - t' - \tau) \\ & + \Theta(t' - t)\delta(t - t' + \tau)), \quad (10) \end{aligned}$$

where μ, η are cavity indices (A or B). The coupling strength is given by $V_{\mu\eta} = (1 + \delta_{\mu\eta})\gamma_1/2$ with the cavity decay rate γ_1 . Due to topology, the inter-cavity coupling is exactly half the dissipation rate. For the 1D case, a photon emitted away from the other cavity will not return, while a photon emitted towards the other cavity can be transferred into that cavity. In higher dimensions, the inter-cavity coupling will be much smaller than the dissipation rate. The delay time τ in Eq. (10) depends implicitly on the involved cavities, with $\tau = R/c$, $\mu \neq \eta$, and 0 otherwise. For one initial excitation, three system states $|A\rangle = |10\rangle$, $|B\rangle = |01\rangle$, $|0\rangle = |00\rangle$ contribute, with

the excitation in slab A or B, or both slabs in the ground state, respectively. Inserting Eq. (10) into Eq. (4) yields the equations of motion. As an example, the occupation in slab A $\langle A|\rho_s(t)|A\rangle$ evolves as (cf. [49]):

$$\begin{aligned} \partial_t \langle A|\rho_s(t)|A\rangle = & -2\gamma_A \langle A|\rho_s(t)|A\rangle \\ & - 2V_{BA}^* e^{-i\omega_B \tau} \langle 0|\rho_{s,0B}^{(1)L}(t, t - \tau)|A\rangle + \text{c.c.} \quad (11) \end{aligned}$$

For the auxiliary density matrix $\rho^{(1)}$, starting from Eq. (9) results in (cf. [49]):

$$\begin{aligned} \partial_t \langle 0|\rho_{s,0B}^{(1)L}(t, t_1)|A\rangle = & \delta(t - t_1) \langle B|\rho_s(t_1)|A\rangle \\ = & -\gamma_A \langle 0|\rho_{s,0B}^{(1)L}(t, t_1)|A\rangle \\ & - 2V_{BA} e^{i\omega_B \tau} \langle B|\rho_{s,B0}^{(1)R}(t_1, t - \tau)|0\rangle \\ & - 2V_{BA} e^{i\omega_A \tau} \langle 0|\rho_{s,0B}^{(1)L}(t - \tau, t_1)|A\rangle. \quad (12) \end{aligned}$$

The remaining equations for the occupation in B, the coherences, and matrix elements for $\rho^{(1)}$ are calculated analogously (cf. [49]). For time-non-local interactions, the system density matrix in Eq. (11) only couples to the first auxiliary density matrix $\rho^{(1)}$. Time-local processes such as the cavity photon dissipation are included in the zeroth step of the hierarchy.

Fig. 2(a) shows the time dynamics of the single-photon occupations in slabs A and B. The model system allows a calculation using the wave function (cf. [49]) as a benchmark. The HEOM (solid lines) and exact wave function (dotted lines) results agree perfectly. Note, that the HEOM allows in principle the inclusion of Lindblad terms (e.g. for pumping), which the wave function does not. Over time the single excitation in slab A will dissipate into the bath. However, some photons are transferred to the QNM of slab B with delay $\tau \approx 44$ ps. For the used parameters, the occupation in B is even larger than the occupation in A after some time. Eventually, the system arrives at a trapped state [14, 50–55] due to constructive interference from the inter-cavity transfer.

Note, that the HEOM allows in principle the inclusion of Lindblad terms (e.g. for pumping), which the wave function does not. Also an extension to two photon processes is feasible for the HEOM. Fig. 2(b) shows the two-photon coherences (two photons on one side of the density matrix, none on the other) for the two slabs from Fig. 1(b), which includes at most two traveling photons, resulting in a calculation analogous to Fig. 2(a). The amplitudes of the intra-cavity coherences $\langle 20|\rho_s|00\rangle/\langle 02|\rho_s|00\rangle$ resemble the dynamics of the densities in Fig. 2(a), since in principle the same independent processes are involved. The inter-cavity coherence $\langle 11|\rho_s|00\rangle$ requires the transfer of just one photon and thus shows a rapid increase after $t = \tau$. In the final equilibrium state the probability (coherence squared) of an inter-cavity contribution matches the sum of the two intra-cavity probabilities.

A feasible calculation of the exact solution as shown here is limited to a small number of photons by the exponential scaling of the numerical complexity with the number of excitations. For systems requiring a higher number of traveling photons, a calculation of the higher steps in the hierarchy via matrix product states or other tensor networks [14, 15, 29–33, 36–40] may be possible as well as analytic calculations in special setups. Furthermore, the HEOM allows a perturbative truncation of the hierarchy for systems with a small system-bath coupling. Thus, at least an approximate solution may be possible for higher excitation numbers.

In conclusion, we analyzed the derivation of hierarchical equations of motion and transferred the idea to open quantum systems with delay. The resulting equations allow a natural, easy truncation on the number of excitations in the bath, which is otherwise cumbersome for Nakajima-Zwanzig or time convolution-less equations. The first implementation for single- and multi-photon transfer between two cavities demonstrated the feasibility of the approach. We expect that in the future more demanding implementations including tensor network approaches may allow the simulation of several photons traveling through complex quantum networks.

* marten.richter@tu-berlin.de

- [1] Y. Tanimura and R. Kubo, Time evolution of a quantum system in contact with a nearly gaussian-markoffian noise bath, *Journal of the Physical Society of Japan* **58**, 101 (1989).
- [2] Y. Tanimura, Numerically “exact” approach to open quantum dynamics: The hierarchical equations of motion (heom), *The Journal of chemical physics* **153**, 020901 (2020).
- [3] L. Ye, X. Wang, D. Hou, R.-X. Xu, X. Zheng, and Y. Yan, Heom-quick: a program for accurate, efficient, and universal characterization of strongly correlated quantum impurity systems, *WIREs Computational Molecular Science* **6**, 608 (2016).
- [4] N. Lambert, T. Raheja, S. Ahmed, A. Pitchford, and F. Nori, Bofin-heom: A bosonic and fermionic numerical hierarchical-equations-of-motion library with applications in light-harvesting, quantum control, and single-molecule electronics, *arXiv preprint arXiv:2010.10806* (2020).
- [5] T. Kramer, M. Noack, A. Reinefeld, M. Rodríguez, and Y. Zelinsky, Efficient calculation of open quantum system dynamics and time-resolved spectroscopy with distributed memory heom (dm-heom), *Journal of Computational Chemistry* **39**, 1779 (2018).
- [6] J. Seibt and O. Kühn, Strong exciton-vibrational coupling in molecular assemblies. dynamics using the polaron transformation in heom space, *The Journal of Physical Chemistry A* **125**, 7052 (2021).
- [7] T. Kramer, M. Noack, J. R. Reimers, A. Reinefeld, M. Rodríguez, and S. Yin, Energy flow in the photosystem i supercomplex: Comparison of approximative theories with dm-heom, *Chemical Physics* **515**, 262 (2018).
- [8] R. F. Oulton, V. J. Sorger, D. Genov, D. Pile, and X. Zhang, A hybrid plasmonic waveguide for subwavelength confinement and long-range propagation, *Nature Photonics* **2**, 496 (2008).
- [9] M. I. Stockman, Nanofocusing of optical energy in tapered plasmonic waveguides, *Physical review letters* **93**, 137404 (2004).
- [10] A. Orieux, M. A. Versteegh, K. D. Jöns, and S. Ducci, Semiconductor devices for entangled photon pair generation: a review, *Reports on Progress in Physics* **80**, 076001 (2017).
- [11] M. Weiß and H. J. Krenner, Interfacing quantum emitters with propagating surface acoustic waves, *Journal of Physics D: Applied Physics* **51**, 373001 (2018).
- [12] H. Jayakumar, A. Predojević, T. Kauten, T. Huber, G. S. Solomon, and G. Weihs, Time-bin entangled photons from a quantum dot, *Nature communications* **5**, 1 (2014).
- [13] A. Carmele and S. Reitzenstein, Non-markovian features in semiconductor quantum optics: quantifying the role of phonons in experiment and theory, *Nanophotonics* **8**, 655 (2019).
- [14] H. Pichler and P. Zoller, Photonic circuits with time delays and quantum feedback, *Phys. Rev. Lett.* **116**, 093601 (2016).
- [15] O. Kaestle, R. Finsterhoelzl, A. Knorr, and A. Carmele, Continuous and time-discrete non-markovian system-reservoir interactions: Dissipative coherent quantum feedback in liouville space, *Phys. Rev. Research* **3**, 023168 (2021).
- [16] S. Arranz Regidor, G. Crowder, H. Carmichael, and S. Hughes, Modeling quantum light-matter interactions in waveguide qed with retardation, nonlinear interactions, and a time-delayed feedback: Matrix product states versus a space-discretized waveguide model, *Phys. Rev. Research* **3**, 023030 (2021).
- [17] M. Richter and S. Hughes, Enhanced tempo algorithm for quantum path integrals with off-diagonal system-bath coupling: Applications to photonic quantum networks, *Phys. Rev. Lett.* **128**, 167403 (2022).
- [18] A. Caldeira and A. Leggett, Path integral approach to quantum brownian motion, *Physica A* **121**, 587 (1983).
- [19] Y. Tanimura and S. Mukamel, Real-time path-integral approach to quantum coherence and dephasing in nonadiabatic transitions and nonlinear optical response, *Phys. Rev. E* **47**, 118 (1993).
- [20] N. Makri and D. E. Makarov, Tensor propagator for iterative quantum time evolution of reduced density matrices. i. theory, *J. Chem. Phys.* **102**, 4600 (1995).
- [21] N. Makri and D. E. Makarov, Tensor propagator for iterative quantum time evolution of reduced density matrices. ii. numerical methodology, *J. Chem. Phys.* **102**, 4611 (1995).
- [22] A. Vagov, M. D. Croitoru, M. Glässl, V. M. Axt, and T. Kuhn, Real-time path integrals for quantum dots: Quantum dissipative dynamics with superohmic environment coupling, *Phys. Rev. B* **83**, 094303 (2011).
- [23] A. Strathearn, B. W. Lovett, and P. Kirton, Efficient real-time path integrals for non-markovian spin-boson models, *New Journal of Physics* **19**, 093009 (2017).
- [24] A. Strathearn, P. Kirton, D. Kilda, J. Keeling, and B. W. Lovett, Efficient non-markovian quantum dynamics using time-evolving matrix product operators, *Nature commu-*

nications **9**, 3322 (2018).

[25] D. Gribben, D. M. Rouse, J. Iles-Smith, A. Strathearn, H. Maguire, P. Kirton, A. Nazir, E. M. Gauger, and B. W. Lovett, Exact dynamics of nonadditive environments in non-markovian open quantum systems, PRX Quantum **3**, 010321 (2022).

[26] M. Cygorek, M. Cosacchi, A. Vagov, V. M. Axt, B. W. Lovett, J. Keeling, and E. M. Gauger, Simulation of open quantum systems by automated compression of arbitrary environments, Nature Physics , 1 (2022).

[27] J. Prior, I. de Vega, A. W. Chin, S. F. Huelga, and M. B. Plenio, Quantum dynamics in photonic crystals, Phys. Rev. A **87**, 013428 (2013).

[28] F. Caycedo-Soler, A. Mattioni, J. Lim, T. Renger, S. Huelga, and M. Plenio, Exact simulation of pigment-protein complexes unveils vibronic renormalization of electronic parameters in ultrafast spectroscopy, Nature Communications **13**, 1 (2022).

[29] S. R. Clark, J. Prior, M. J. Hartmann, D. Jaksch, and M. B. Plenio, Exact matrix product solutions in the Heisenberg picture of an open quantum spin chain, New Journal of Physics **12**, 025005 (2010).

[30] A. H. Werner, D. Jaschke, P. Silvi, M. Kliesch, T. Calarco, J. Eisert, and S. Montangero, Positive tensor network approach for simulating open quantum many-body systems, Phys. Rev. Lett. **116**, 237201 (2016).

[31] R. Rosenbach, J. Cerrillo, S. F. Huelga, J. Cao, and M. B. Plenio, Efficient simulation of non-markovian system-environment interaction, New Journal of Physics **18**, 023035 (2016).

[32] F. A. Schröder, D. H. Turban, A. J. Musser, N. D. Hine, and A. W. Chin, Tensor network simulation of multi-environmental open quantum dynamics via machine learning and entanglement renormalisation, Nature communications **10**, 1 (2019).

[33] A. D. Somoza, O. Marty, J. Lim, S. F. Huelga, and M. B. Plenio, Dissipation-assisted matrix product factorization, Phys. Rev. Lett. **123**, 100502 (2019).

[34] V. Chernyak and S. Mukamel, Collective coordinates for nuclear spectral densities in energy transfer and femtosecond spectroscopy of molecular aggregates, J. Chem. Phys. **105**, 4565 (1996), <https://doi.org/10.1063/1.472302>.

[35] M. Richter and A. Knorr, A time convolution less density matrix approach to the nonlinear optical response of a coupled system-bath complex, Annals of Physics **325**, 711 (2010).

[36] R. Orús, A practical introduction to tensor networks: Matrix product states and projected entangled pair states, Annals of Physics **349**, 117 (2014).

[37] U. Schollwöck, The density-matrix renormalization group in the age of matrix product states, Annals of physics **326**, 96 (2011).

[38] J. Cirac, D. Pérez-García, N. Schuch, and F. Verstraete, Matrix product density operators: Renormalization fixed points and boundary theories, Annals of Physics **378**, 100 (2017).

[39] F. Verstraete and J. I. Cirac, Matrix product states represent ground states faithfully, Physical Review B **73**, 094423 (2006).

[40] G. Vidal, Classical simulation of infinite-size quantum lattice systems in one spatial dimension, Physical review letters **98**, 070201 (2007).

[41] H.-P. Breuer, F. Petruccione, *et al.*, *The theory of open quantum systems* (Oxford University Press on Demand, 2002).

[42] G. García-Calderón and R. Peierls, Resonant states and their uses, Nuclear Physics A **265**, 443 (1976).

[43] K. Lee, P. Leung, and K. Pang, Dyadic formulation of morphology-dependent resonances. i. completeness relation, JOSA B **16**, 1409 (1999).

[44] E. A. Muljarov, W. Langbein, and R. Zimmermann, Brillouin-wigner perturbation theory in open electromagnetic systems, EPL (Europhysics Letters) **92**, 50010 (2011).

[45] P. T. Kristensen, C. Van Vlack, and S. Hughes, Generalized effective mode volume for leaky optical cavities, Optics letters **37**, 1649 (2012).

[46] C. Sauvan, J.-P. Hugonin, I. S. Maksymov, and P. Lalanne, Theory of the spontaneous optical emission of nanosize photonic and plasmon resonators, Physical Review Letters **110**, 237401 (2013).

[47] S. Franke, S. Hughes, M. K. Dezfouli, P. T. Kristensen, K. Busch, A. Knorr, and M. Richter, Quantization of quasinormal modes for open cavities and plasmonic cavity quantum electrodynamics, Physical review letters **122**, 213901 (2019).

[48] P. T. Kristensen, K. Herrmann, F. Intravaia, and K. Busch, Modeling electromagnetic resonators using quasinormal modes, Advances in Optics and Photonics **12**, 612 (2020).

[49] See supplemental material at [url will be inserted by publisher] for (i) analytic coupling elements,(ii) equations of motions and (iii) approach using the wave function.

[50] M. Bello, G. Platero, J. I. Cirac, and A. González-Tudela, Unconventional quantum optics in topological waveguide qed, Science advances **5**, eaaw0297 (2019).

[51] S. Hughes and G. S. Agarwal, Anisotropy-induced quantum interference and population trapping between orthogonal quantum dot exciton states in semiconductor cavity systems, Physical review letters **118**, 063601 (2017).

[52] A. L. Grimsmo, Time-delayed quantum feedback control, Physical review letters **115**, 060402 (2015).

[53] N. Német, A. Carmele, S. Parkins, and A. Knorr, Comparison between continuous-and discrete-mode coherent feedback for the jaynes-cummings model, Physical Review A **100**, 023805 (2019).

[54] K. Barkemeyer, R. Finsterhözl, A. Knorr, and A. Carmele, Revisiting quantum feedback control: disentangling the feedback-induced phase from the corresponding amplitude, Advanced Quantum Technologies **3**, 1900078 (2020).

[55] R. Finsterhözl, M. Katzer, and A. Carmele, Nonequilibrium non-markovian steady states in open quantum many-body systems: Persistent oscillations in heisenberg quantum spin chains, Physical Review B **102**, 174309 (2020).

[56] P. Lalanne, W. Yan, K. Vynck, C. Sauvan, and J.-P. Hugonin, Light interaction with photonic and plasmonic resonances, Laser & Photonics Reviews **12**, 1700113 (2018).

[57] R.-C. Ge, P. T. Kristensen, J. F. Young, and S. Hughes, Quasinormal mode approach to modelling light-emission and propagation in nanoplasmonics, New Journal of Physics **16**, 113048 (2014).

[58] S. Franke, M. Richter, J. Ren, A. Knorr, and S. Hughes, Quantized quasinormal-mode description of nonlinear

cavity-qed effects from coupled resonators with a fano-like resonance, Physical Review Research **2**, 033456 (2020).

[59] T. Gruner and D.-G. Welsch, Green-function approach to the radiation-field quantization for homogeneous and inhomogeneous kramers-kronig dielectrics, Phys. Rev. A **53**, 1818 (1996).

[60] S. Mukamel, *Principles of nonlinear optical spectroscopy*, 6 (Oxford University Press on Demand, 1999).

Analytic coupling elements

We use analytic expressions of the mode frequencies, decay constants, and coupling elements for numeric evaluation. For linearly polarized waves and assuming a homogeneous continuation in y, z -direction, the problem reduces to the 1D model from Fig. 1(b). The QNM within each slab is given by [48, 56]

$$\tilde{f}_\mu(x) \Big|_{|x| < L/2} = e^{i n_R k_\mu x} + e^{-i n_R k_\mu x + i \mu \pi}, \quad (\text{S1})$$

where $n_R = \sqrt{\epsilon_R}$ is the refractive index of the slab and $k_\mu = \tilde{\omega}_\mu/c$ is the QNM wavenumber. The QNM frequency $\tilde{\omega}_\mu$ is [48, 56]

$$\tilde{\omega}_\mu L/c = \frac{2\pi\mu + i \ln((n_R - n_B)^2/(n_r + n_B)^2)}{2n_R}. \quad (\text{S2})$$

Thus, the frequency of the first QNM $\tilde{f}_1(x)$ is $\tilde{\omega}_1 = \omega_1 - i\gamma_1 = (1 - i0.21)L/c$. The second QNM $\tilde{f}_2(x)$ has a resonance frequency that is twice as large. Hence, as a first approximation, we take only the first QNM in our calculations.

Outside of the cavity ($|x| > L/2$), we replace the QNMs with regularized modes [57] $\tilde{F}_\mu(x, \omega) = \int_{-L/2}^{L/2} dx' G_B(x, x', \omega) \Delta\epsilon(x') \tilde{f}_\mu(x') = (x/|x|) M_\mu(\omega) e^{i\omega|x|/c}$, where $\Delta\epsilon(x) = \epsilon_R - \epsilon_B$, $|x| < L/2$, and 0 otherwise, and

$$M_\mu(\omega) = \frac{i}{2} L(\pi^2 - 1) \left[\text{si}\left(\frac{(\omega + \pi\tilde{\omega}_\mu)L}{2c}\right) - \text{si}\left(\frac{(\omega - \pi\tilde{\omega}_\mu)L}{2c}\right) \right] \quad (\text{S3})$$

is an analytical factor that vanishes for $\omega \rightarrow \infty$. $\text{si}(x) = \sin(x)/x$ is the unnormalized sinc-function. $G_B(x, x', \omega) = i e^{-i\omega|x-x'|/c}/2$ is the vacuum Green's function for the case of linearly polarized waves, solving the Helmholtz equation

$$\left(\partial_x^2 + \frac{\omega^2}{c^2} \right) G_B(x, x', \omega) = \frac{\omega^2}{c^2} \delta(x - x'). \quad (\text{S4})$$

We locate the slab A at $x = 0$ and slab B at $x = R$ (cf. Fig. 1(b)), so that $\tilde{f}_1(x) = \tilde{f}_A(x)$ and $\tilde{f}_B(x) = \tilde{f}_A(x - R)$. We quantize the QNMs following the procedure laid out in [47], with minor adjustments due to the 1D nature of the problem, e.g. taking the 1D analog of the electric field quantization and QNM Green function instead of the 3D expressions that were used in [47]. Since the QNM quantization relies on a complex dissipative permittivity, we add a constant imaginary part to the permittivities of the slabs and background medium: $\epsilon^\alpha = \epsilon_{R/B} + i\alpha\kappa$ (cf. [58]) so that the original values are retained in the limit $\alpha \rightarrow 0$. Taking the 1D analog of the quantization

in dissipative media from [59], we find the electric field operator to be

$$E^\alpha(x) = \int_0^\infty d\omega \int dx' \frac{i}{\omega\epsilon_0} G^\alpha(x, x', \omega) \hat{j}^\alpha(x', \omega) + \text{H.a.}, \quad (\text{S5})$$

where $G(x, x', \omega)$ is the Greens function of the dissipative medium and $\hat{j}^\alpha(x, \omega) = \omega\sqrt{(\hbar\epsilon_0/\pi)\epsilon_I^\alpha(x, \omega)}\hat{b}(x, \omega)$ is the noise-current density operator, with ϵ_I denoting the imaginary part of the permittivity and $\hat{b}(x, \omega)$ a Bosonic photon annihilation operator. We use the Green's function expansion in terms of QNMs [43, 56, 57] $G(x, x', \omega) = \sum_{\mu=A,B} A_\mu(\omega) \tilde{f}_\mu(x) \tilde{f}_\mu(x')$, where $A_\mu(\omega) = \omega/(2(\tilde{\omega}_\mu - \omega))$, and the QNM functions \tilde{f}_μ are replaced with regularized modes \tilde{F}_μ outside their respective cavity volumes. Inserting the QNM Green's function into Eq. (S5), we find QNM operators analogous to [47]:

$$\begin{aligned} \tilde{a}_A = & \sqrt{\frac{2}{\pi\omega_A}} \int_0^\infty d\omega A_A(\omega) \\ & \left[\int_{-L/2}^{L/2} dx \sqrt{\epsilon_I^\alpha(x, \omega)} \tilde{f}_A^\alpha(x) \hat{b}(x, \omega) \right. \\ & + \lim_{\lambda \rightarrow \infty} \int_{L/2}^\lambda dx \sqrt{\epsilon_I^\alpha(x, \omega)} \tilde{F}_A^\alpha(x, \omega) \hat{b}(x, \omega) \\ & \left. + \lim_{\lambda \rightarrow \infty} \int_{-\lambda}^{-L/2} dx \sqrt{\epsilon_I^\alpha(x, \omega)} \tilde{F}_A^\alpha(x, \omega) \hat{b}(x, \omega) \right], \end{aligned} \quad (\text{S6})$$

which depend implicitly on $\alpha \rightarrow 0$. In the first integral, the limit $\alpha \rightarrow 0$ can be carried out immediately, so that this contribution vanishes, because $\lim_{\alpha \rightarrow 0} \epsilon_I^\alpha = 0$. In the other two integrals, the order of the limits cannot be exchanged, as pointed out in [58], so the limit $\lambda \rightarrow \infty$ has to be taken first. The operators for the QNMs of cavity B are defined analogously, just spatially shifted by R . The QNM operators defined in Eq. (S6) are non-Bosonic, with $[\tilde{a}_A, \tilde{a}_A^\dagger] = S_{AA}$, and

$$\begin{aligned} S_{AA} = & \frac{2}{\pi\omega_A} \int_0^\infty d\omega A_A(\omega) A_A^*(\omega) \\ & \times \left[\lim_{\lambda \rightarrow \infty} \int_{L/2}^\lambda dx \epsilon_I^\alpha(x, \omega) \tilde{F}_A^\alpha(x, \omega) \tilde{F}_A^{*,\alpha}(x, \omega) \right. \\ & \left. + \lim_{\lambda \rightarrow \infty} \int_{-\lambda}^{-L/2} dx \epsilon_I^\alpha(x, \omega) \tilde{F}_A^\alpha(x, \omega) \tilde{F}_A^{*,\alpha}(x, \omega) \right]. \end{aligned} \quad (\text{S7})$$

Analogous to [58], we employ the Helmholtz equation of the background Green's function (Eq. (S4)) to reduce the integral over x to the value of the modes at the limits of the integration volume. Taking the limit $\lambda \rightarrow \infty$ first and then $\alpha \rightarrow 0$, we find

$$S_{AA} = \frac{2c}{\gamma_1} |M_1(\tilde{\omega}_1)|^2, \quad (\text{S8})$$

where we used $\tilde{\omega}_A = \tilde{\omega}_1$.

The overlap integral $[\tilde{a}_A, \tilde{a}_B^\dagger] = S_{AB}$ is calculated accordingly. We make use of the fact that the two slabs are identical except for their spatial separation and hence $\tilde{\omega}_A = \tilde{\omega}_B = \tilde{\omega}_1$, to obtain

$$S_{AB} = \frac{2c}{\gamma_1} |M_1(\tilde{\omega}_1)|^2 \operatorname{Re} \left\{ \frac{\tilde{\omega}_1}{2\omega_1} e^{-i\omega_1 R/c} \right\} e^{-\gamma_1 R/c}. \quad (\text{S9})$$

Since $|\operatorname{Re} \{ \tilde{\omega}_1 e^{-i\omega_1 R/c} / (2\omega_1) \}| < 1$, it follows that $|S_{AB}/S_{AA}| < e^{-\gamma_1 R/c}$, due to the retarded interaction between the slabs. The QNMs penetrate through the boundary of the slab so that there is a non-zero overlap even without time delay. However, the mode is concentrated at the cavity so that the overlap is small if the slabs are well enough separated. Below, the correlation functions are discussed for the case with finite time delay. The QNMs' wavelength is $\lambda_1 = 2L$, so a separation of a few dozen wavelengths, as used in the main text, leads to negligible contributions of the overlap.

Thus, the QNM operators are symmetrized independently within their respective cavities similar to the single-cavity case in [47]:

$$\hat{a}_\mu = \int dx \int_0^\infty d\omega L_\mu(x, \omega) \hat{b}(x, \omega), \quad (\text{S10})$$

with

$$L_\mu(x, \omega) = S_{\mu\mu}^{-1/2} \sqrt{\frac{\gamma_\mu \epsilon_I(x, \omega)}{\pi c \omega_\mu |M_1(\tilde{\omega}_\mu)|}} A_\mu(\omega) \tilde{f}_\mu(x), \quad (\text{S11})$$

and the mode function \tilde{f}_μ is replaced by the regularized mode \tilde{F}_μ outside the slab volume. The imaginary part of the permittivity and the bounds of the spatial integral include implicit limits, as discussed above.

We now define continuum operators $\hat{c}(x, \omega) = \hat{b}(x, \omega) - \sum_{\mu=A,B} L_\mu^*(x, \omega) \hat{a}_\mu$ [58], which commute with the symmetrized Bosonic QNM operators and serve as the bath. While they are generally non-Bosonic, as a first approximation, we neglect the non-Bosonic contributions. This allows us to decompose the full Hamiltonian $H = \hbar \int dx \int_0^\infty d\omega \omega \hat{b}^\dagger(x, \omega) \hat{b}(x, \omega)$ into system and bath parts [58]:

$$\begin{aligned} H_S &= \hbar \sum_{\mu=A,B} \omega_\mu \hat{a}_\mu^\dagger \hat{a}_\mu, \\ H_B &= \hbar \int dx \int_0^\infty d\omega \omega \hat{c}^\dagger(x, \omega) \hat{c}(x, \omega), \\ H_{SB} &= \hbar \sum_{\mu=A,B} \int dx \int_0^\infty d\omega g_\mu(x, \omega) \hat{c}(x, \omega) \hat{a}_\mu^\dagger + \text{H.a.} \end{aligned} \quad (\text{S12})$$

The coupling elements $g_\mu(x, \omega) = -S_{\mu\mu}^{-1/2} \times \sqrt{\epsilon_I(x, \omega) / (2\pi\omega_\mu)} \omega \tilde{f}_\mu(x)$, are derived from the projectors $L_\mu(x, \omega)$, with the pole at $\omega = \tilde{\omega}_\mu$ removed

during the derivation, as shown in [58].

To derive the coupling strength of the interaction between the slabs mediated via the bath, we calculate the correlation function [34, 60] that characterizes the system-bath interaction in the HEOM formalism:

$$\begin{aligned} C_{\mu\eta}(t - t') &= \hbar^2 \int_0^\infty d\omega \int_0^\infty d\omega' \int dx \int dx' e^{-i\omega(t-t')} \\ &\quad \times g_\mu(x, \omega) g_\eta^*(x', \omega') \langle \hat{c}(x, \omega) \hat{c}^\dagger(x', \omega') \rangle_B. \end{aligned} \quad (\text{S13})$$

For $\rho_B = |0\rangle\langle 0|$ (no initial photons), the trace results in a delta function, so only an integral over the coupling elements remains. This is calculated similarly to [58], i.e. by assuming that the coupling is sharply peaked at the QNM frequency, so that

$$\begin{aligned} \int dx g_\mu(x, \omega) g_\eta^*(x, \omega) &\approx S_{11}^{-1} \frac{2c}{\gamma_1} |M_1(\tilde{\omega}_1)|^2 \frac{\gamma_1}{2\pi} \\ &\quad \times \left(e^{i\omega R_{\mu\eta}/c} + e^{-i\omega R_{\mu\eta}/c} \right), \end{aligned} \quad (\text{S14})$$

where $|R_{\mu\eta}|$ is R if $\mu \neq \eta$ and 0 otherwise. Using $S_{11} = 2c|M_1(\tilde{\omega}_1)|^2/\gamma_1$, and defining the retardation time $\tau = R_{\mu\eta}/c$ as an implicit function of μ and η , the correlation function becomes

$$C_{\mu\eta}(t - t') = \frac{\gamma_1 \hbar^2}{2\pi} \int_0^\infty d\omega (e^{i\omega\tau} + e^{-i\omega\tau}) e^{-i\omega(t-t')}, \quad (\text{S15})$$

As a final approximation, we extend the lower limit to $-\infty$ [58], to obtain the correlation function in Eq. (10).

Calculation of the equations of motion

For equations of motion of the density-matrix elements, we convert Eq. (4) to a more explicit form by replacing the indices $l \rightarrow (\alpha, \nu_1 \nu_2, x, \omega)$ of the system and bath operators

$$\begin{aligned} A_l(t) &\rightarrow \hat{A}_{\nu_1 \nu_2}^\alpha(t), \\ B_l(t) &\rightarrow \sum_\mu \langle \nu_1 | \hat{a}_\mu | \nu_2 \rangle \int dx \int_0^\infty d\omega g_\mu^*(x, \omega) \hat{c}^{\dagger, \alpha}(x, \omega) + \text{H.a.}, \end{aligned} \quad (\text{S16})$$

with $\hat{A}_{\nu_1 \nu_2} = |\nu_1\rangle\langle \nu_2|$, so that

$$\begin{aligned} \partial_t \rho_s(t) &= -\frac{i}{\hbar} H_{s,-}(t) \rho_s(t) \\ &\quad + \sum_{\alpha, \beta=L, R} \sum_{\nu_1 \dots \nu_4} (-1)^{\alpha+\beta} \hat{A}_{\nu_1 \nu_2}^\alpha(t) \\ &\quad \times \int_{t_0}^t dt_1 C_{\nu_1 \nu_2 \nu_3 \nu_4}^{\beta}(t, t_1) \rho_{s, \nu_3 \nu_4}^{(1)\beta}(t, t_1), \end{aligned} \quad (\text{S17})$$

where $|\nu_i\rangle$ is a system state, and α, β determines whether the operator acts on the left or right side of the density matrix. The sign is negative if $\alpha \neq \beta$. The correlation function is defined as $C_{\nu_1 \nu_2 \nu_3 \nu_4}^L(t, t_1) = \sum_{\mu\eta} \langle \nu_1 | \hat{a}_\mu^\dagger | \nu_2 \rangle \langle \nu_3 | \hat{a}_\eta | \nu_4 \rangle C_{\mu\eta}(t - t_1)$, with $C_{\mu\eta}$ from Eq. (10), and $C_{\nu_1 \nu_2 \nu_3 \nu_4}^R(t, t_1) = (C_{\nu_1 \nu_2 \nu_3 \nu_4}^L(t, t_1))^*$. For brevity, we use $|A\rangle, |B\rangle, |0\rangle$ as defined in the main text, above Eq. (11). To derive Eq. (11), we take the expectation value with respect to state $|A\rangle$ on (S17) to obtain,

$$\begin{aligned} \partial_t \langle A | \rho_s(t) | A \rangle &= -\frac{i}{\hbar} \langle A | H_{s,-} \rho_s(t) | A \rangle \\ &+ \sum_{\alpha, \beta=L, R} \sum_{\nu_1 \dots \nu_4} (-1)^{\alpha+\beta} \int_{t_0}^t dt_1 C_{\nu_1 \nu_2 \nu_3 \nu_4}^\beta(t, t_1) \\ &\quad \times \langle A | \hat{A}_{\nu_1 \nu_2}^\alpha(t) \rho_{s, \nu_3 \nu_4}^{(1)\beta}(t, t_1) | A \rangle. \end{aligned} \quad (\text{S18})$$

Since the $|\nu_i\rangle$ are orthogonal, only certain combinations of states and α, β survive. Using the definition of the QNM correlation function (Eq. (10)) and the initial conditions for $\rho^{(1)}$, results in the first-order equation of motion given in Eq. (11). Similarly, we obtain an equation for the coherence $\langle A | \rho_s(t) | B \rangle$:

$$\begin{aligned} \partial_t \langle A | \rho_s(t) | B \rangle &= -(\gamma_A + \gamma_B) \langle A | \rho_s(t) | B \rangle \\ &- 2V_{BA}^* e^{-i\omega_B \tau} \langle 0 | \rho_{s,0B}^{(1)L}(t, t - \tau) | B \rangle \\ &\quad + \text{c.c.} (A \leftrightarrow B). \end{aligned} \quad (\text{S19})$$

The equations for the occupation in slab B and the second coherence term are obtained from Eq. (11) and Eq. (S19), respectively, by exchanging $A \leftrightarrow B$. For Eq. (12), we insert Eq. (S16) into Eq. (9). We use a rotating-frame representation of $\rho^{(1)}$ with respect to its time arguments, e.g.,

$$\langle 0 | \rho_{s,0B}^{(1),L}(t, t_1) | A \rangle \rightarrow e^{-i\omega_1(t+t_1)} \langle 0 | \rho_{s,0B}^{(1),L}(t, t_1) | A \rangle, \quad (\text{S20})$$

where we have used $\omega_A = \omega_B = \omega_1$. A similar derivation as for the matrix elements of ρ_s yields fast-rotating terms. Within the rotating-frame, $\langle 0 | \rho_{s,0B}^{(1),L}(t, t_1) | A \rangle$ evolves according to Eq. (12). In the same manner, we derive:

$$\begin{aligned} \partial_t \langle A | \rho_{s,A0}^{(1)R}(t, t_1) | 0 \rangle &= \delta(t - t_1) \langle A | \rho_s(t_1) | A \rangle \\ &= -\gamma_A \langle A | \rho_{s,A0}^{(1)L}(t, t_1) | 0 \rangle \\ &- 2V_{BA}^* e^{-i\omega_B \tau} \langle 0 | \rho_{s,0B}^{(1)R}(t_1, t - \tau) | A \rangle \\ &- 2V_{BA}^* e^{-i\omega_B \tau} \langle B | \rho_{s,A0}^{(1)L}(t - \tau, t_1) | 0 \rangle. \end{aligned} \quad (\text{S21})$$

The last six matrix elements of $\rho^{(1)}$ are derived from Eq. (12) and (S21) by complex conjugation or exchanging the indices A and B . Note that $\rho^{(1)}(t, t_1)$ vanishes for $t < t_1$ or $t_1 < 0$. Furthermore, only $\rho^{(1)}(t, t - \tau)$ appears

in Eq. (11) and Eq. (S19). Therefore, the last terms in Eq. (12) and Eq. (S21), respectively, do not contribute to the dynamics of ρ_s .

For the two-photon coherences, we obtain (following a similar derivation as for the single-photon occupation):

$$\begin{aligned} \partial_t \langle 20 | \rho_s(t) | 00 \rangle &= -2\gamma_A \langle 20 | \rho_s(t) | 00 \rangle \\ &- \sqrt{8}V_{BA}^* e^{-i\omega_A \tau} \langle 10 | \rho_{s,0B1B}^{(1)L}(t, t - \tau) | 00 \rangle, \end{aligned} \quad (\text{S22})$$

where we use 0_B and 1_B to indicate that the initial system-bath interaction involves the transition of cavity B from the one-photon state to the ground state. Analogously, $\langle 02 | \rho_s(t) | 00 \rangle = (\langle 20 | \rho_s(t) | 00 \rangle)(A \leftrightarrow B)$ and

$$\begin{aligned} \partial_t \langle 11 | \rho_s(t) | 00 \rangle &= -(\gamma_A + \gamma_B) \langle 11 | \rho_s(t) | 00 \rangle \\ &- \sqrt{8}V_{BA}^* e^{-i\omega_A \tau} \langle 01 | \rho_{s,1B2B}^{(1)L}(t, t - \tau) | 00 \rangle \\ &- \sqrt{8}V_{AB}^* e^{-i\omega_B \tau} \langle 10 | \rho_{s,1A2A}^{(1)L}(t, t - \tau) | 00 \rangle \\ &- 2V_{BA}^* e^{-i\omega_A \tau} \langle 01 | \rho_{s,0B1B}^{(1)L}(t, t - \tau) | 00 \rangle \\ &- 2V_{AB}^* e^{-i\omega_B \tau} \langle 10 | \rho_{s,0A1A}^{(1)L}(t, t - \tau) | 00 \rangle. \end{aligned} \quad (\text{S23})$$

The equations for the matrix elements of $\rho^{(1)}$ in the rotating frame read (keeping only those terms that contribute to ρ_s):

$$\begin{aligned} \partial_t \langle 10 | \rho_{s,0B1B}^{(1)L}(t, t_1) | 00 \rangle &= \delta(t - t_1) \partial_t \langle 11 | \rho_s(t_1) | 00 \rangle \\ &- \gamma_A \langle 10 | \rho_{s,0B1B}^{(1)L}(t, t_1) | 00 \rangle \\ &- \sqrt{8}V_{BA}^* e^{-i\omega_A \tau} \langle 01 | \rho_{s,1B2B}^{(1)L}(t_1, t - \tau) | 00 \rangle \\ &- 2V_{BA}^* e^{-i\omega_A \tau} \langle 01 | \rho_{s,0B1B}^{(1)L}(t_1, t - \tau) | 00 \rangle, \\ \partial_t \langle 10 | \rho_{s,0A1A}^{(1)L}(t, t_1) | 00 \rangle &= -\gamma_A \langle 10 | \rho_{s,0A1A}^{(1)L}(t, t_1) | 00 \rangle \\ &- 2V_{BA}^* e^{-i\omega_A \tau} \langle 10 | \rho_{s,0B1B}^{(1)L}(t_1, t - \tau) | 00 \rangle, \\ \partial_t \langle 10 | \rho_{s,1A2A}^{(1)L}(t, t_1) | 00 \rangle &= \delta(t - t_1) \partial_t \langle 20 | \rho_s(t_1) | 00 \rangle \\ &- \gamma_A \langle 10 | \rho_{s,1A2A}^{(1)L}(t, t_1) | 00 \rangle. \end{aligned} \quad (\text{S24})$$

The remaining three matrix elements are again obtained by exchanging $A \leftrightarrow B$.

Wave function approach

For initially one excitation in slab A from Fig. 1(b), the general wave function has the form

$$|\psi\rangle = N_A |A\rangle |0\rangle + N_B |B\rangle |0\rangle + \int dx \int_0^\infty d\omega N_{x,\omega} |0\rangle |x, \omega\rangle. \quad (\text{S25})$$

The first Ket refers to the system state as defined above Eq. (11), and the second is the bath state with continuous spatial and frequency indices x, ω . N is the time-dependent amplitude of a particular state, with the initial conditions $N_A(0) = 1$, $N_B(0) = N_{x,\omega}(0) = 0$. In the

interaction picture, the dynamics of the states are governed by the Schrödinger equation with the system-bath interaction Hamiltonian from Eq. (S12). The QNM and bath operators carry the free evolution of the system and bath: $\hat{a}_\mu(t) = e^{-i\omega_\mu t} \hat{a}_\mu$ and $\hat{c}(x, \omega, t) = e^{-i\omega t} \hat{c}(x, \omega)$.

Multiplying the Schrödinger equation for (S25) with $\langle 0 | \langle A |$ from the left yields an equation for N_A :

$$i\hbar \partial_t N_A(t) = \hbar \int dx \int_0^\infty d\omega N_{x,\omega} g_A(x, \omega) e^{-i\omega t} e^{i\omega_A t}. \quad (\text{S26})$$

Similarly, we obtain the equation for $N_{x,\omega}$:

$$i\hbar \partial_t N_{x,\omega}(t) = \hbar (N_A g_A^*(x, \omega) e^{-i\omega_A t} + N_B g_B^*(x, \omega) e^{-i\omega_B t}) e^{i\omega t},$$

which we integrate formally and insert the result back into eq. (S26) to find:

$$\begin{aligned} \partial_t N_A(t) = -\frac{1}{\hbar^2} \int_{t_0}^\infty dt' \int dx \int_0^\infty d\omega (C_{AA}(t-t') N_A(t') \\ + e^{i\omega_A t - i\omega_B t'} C_{AB}(t-t') N_B(t')), \end{aligned} \quad (\text{S27})$$

where we have inserted the definition of the QNM correlation function from Eq. (S13). Using Eq. (10) and $\omega_A = \omega_B$, we arrive at:

$$\partial_t N_A(t) = -\gamma_A N_A(t) - 2V_{BA}^* e^{i\omega_B \tau} N_B(t-\tau) \Theta(t-\tau). \quad (\text{S28})$$

An analogous derivation for N_B yields a similar equation, with the indices switched ($A \leftrightarrow B$). The density matrix elements are calculated by multiplying the amplitudes with their complex conjugates, e.g., $\langle A | \rho_s | A \rangle = |N_A|^2$.